Geol. Mag. **143** (*4*), *2006, pp. 491–508.* © *2006 Cambridge University Press*
doi:10.1017/S0016756806001981 *Printed in the United Kingdom*

Variscan veins: record of fluid circulation and Variscan tectonothermal events in Upper Palaeozoic limestones of the Moravian Karst, Czech Republic

M. SLOBODNÍK*, PH. MUCHEZ†, J. KRÁL‡ & E. KEPPENS§

*Institute of Geological Sciences, Masaryk University, Kotlářská 2, 611 37 Brno, Czech Republic
†Afd. Fysico-chemische Geologie, Katholieke Universiteit Leuven, Celestijnenlaan 200C, B-3001 Leuven, Belgium
‡Geological Survey of Slovak Republic, Mlynská dolina 1, 817 04 Bratislava, Slovak Republic
§Laboratorium voor Geochronology, Vrije Universiteit Brussel, Pleinlaan 2, B-1050, Belgium

(*Received* 23 November 2004; *revised version received* 6 October 2005; *accepted* 17 October 2005)

Abstract – Numerous Variscan syntectonic calcite veins cross-cut Palaeozoic rocks in the Moravian Karst. A structural, petrographic and stable isotopic analysis of the calcite veins and a microthermometric study of fluid inclusions in these vein cements have been carried out to determine the origin of the Variscan fluids and their migration during burial and deformation. The isotopic parameters of white (older, more deformed) and rose (younger) calcites are: $^{87}Sr/^{86}Sr$ is between 0.7078 and 0.7082 (white) and 0.7086 (rose), $\delta^{18}O$ is between +17.7 and +26.1 (white) and between +14.8 and +20.7 ‰ SMOW (rose), $\delta^{13}C$ ranges from +0.1 to +2.5 (white) and from −0.3 to +1.6 ‰ V-PDB (rose). The isotopic signatures point to precipitation in an older fluid system buffered by the host rock (white calcites) and to an open, younger fluid-dominated system (rose calcites). Parent fluids (H_2O–NaCl system) had salinities between 0.35 and 17.25 eq. wt % NaCl. The pressure-corrected and confined homogenization temperatures suggest formation of the calcite veins from a fluid with a temperature between 120 and 170 °C, a pressure of 300–880 bar at a depth between 2.1 and 3.2 km. The fluids were most likely confined to a particular sedimentary bed as a bed-scale fluid migration (white older calcite veins) or, later, to a pile of Palaeozoic sediments as a stratigraphically restricted fluid flow (rose younger calcite veins). The low temperatures and pressures during precipitation of calcites, which took place close to a peak of burial/deformation, confirm the distal position of the Moravian Karst region within the Variscan orogen.

Keywords: Palaeozoic, calcite, veins, syntectonic processes, fluid dynamics.

1. Introduction

Tectonothermal processes can cause the expulsion of basinal pore fluids, resulting in the formation of veins (Muchez *et al.* 1995; Meere & Banks, 1997; Evans & Battles, 1999; Wagner & Cook, 2000; Conti *et al.* 2001; Nemčok *et al.* 2002; Schulz, Audren & Triboulet, 2002). Syntectonic calcite veins in limestones are believed to be a product of diagenesis/low-grade metamorphism and pressure solution (e.g. Ramsay & Huber, 1987). Syntectonic veins can form from fluids in a closed or open geochemical system; a general discussion on open versus closed fluid systems is given by Gregory & Criss (1986). Rock-buffered veins (Gray, Gregory & Durney, 1991) precipitate under the dominant influence of the host rock, and the isotopic composition of the veins is similar to that of the host rock and results from an isotopic equilibrium between the fluid and the rock mass. If the fluids were, however, unable to completely isotopically equilibrate with the rocks, due to relatively rapid flow or being confined to fractures, they carry the signature of original fluid source (Cartwright & Buick, 2000). Rock-buffered fluids are associated with small-scale closed systems where dissolution–precipitation creep is the most likely mechanism for veining, particularly in carbonates (Cartwright & Buick, 2000; Oliver & Bons, 2001).

In open fluid systems, the isotopic composition of the ambient fluid may be out of equilibrium with the solid phases of the rock. Consequently, the isotopic composition of the veins does not reflect that of the host rock (Burkhard & Kerrich, 1988). Open systems are often reported from extensional tectonic regimes (Conti *et al.* 2001), and advection is a dominant fluid flow mechanism for such systems (Jamtveit & Yardley, 1997; Oliver & Bons, 2001). Advection as a mechanism for mass transfer of fluids prevails later in the deformation history of rock, although during early phases, diffusion is more important (Gray, Anastasio & Holl, 2001). Knoop, Kennedy & Dipple (2002) reported evidence for kilometre-scale and outcrop-scale fluid migration based on the study of the $\delta^{18}O$ composition of rock and veins in the Canadian Cordillera. In calcareous sequences, veins systematically exhibited lower $\delta^{18}O$ values than their

*Author for correspondence: marek@sci.muni.cz

host rock, implying modest disequilibrium with the rocks.

Only when the syntectonic fluids are in thermal equilibrium with the host-rock can the microthermometric data of fluid inclusions in syntectonic veins be used to constrain the *P–T* conditions during deformation. If it can be demonstrated that most of the calcite filling of the veins is derived from the host-rock or that chemical equilibrium existed between the ambient fluid and the surrounding rocks, thermal equilibrium between the fluid and rock can be assumed. In this case, it is possible to use microthermometric measurements of assemblages of fluid inclusions in syntectonic veins to study the thermal history during deformation (Fitzgerald *et al.* 1994). A strong positive correlation between the homogenization temperature (T_h) of fluid inclusions and host rock vitrinite reflectance, indicating thermal equilibrium between fluid and rocks, has been demonstrated by earlier studies (e.g. Barker & Goldstein, 1990).

Isotopes, major- and trace-element contents, and Sr-isotopic ratios of the vein carbonates may be used to deduce the fluid origin and to estimate the migration distance of the elements and of the fluid (Janssen *et al.* 1998; Sample & Reid, 1998). Only small-scale fluid migration is reported from calcite veins in shales (the Toarcian shales, the French Massif Central) (Mathieu *et al.* 2000), although large-scale fluid flow has been traced during epigenetic dolomitization by Boni *et al.* (2000). The oxygen isotope exchange (quartz–fluid) has been used to estimate conditions of fluid–rock interaction (O'Hara *et al.* 1997; Schulz Audren & Triboulet, 2002), which could also be enhanced by thrust-related deformation (Abart & Ramseyer, 2002).

Parameters such as illite crystallinity, vitrinite reflectance (R_r), conodont alteration index (CAI), chlorite geothermometry and microthermometry of fluid inclusions have been combined to unravel the palaeothermal evolution of different areas in the Variscan belt (e.g. Leischner, Welte & Littke, 1993; Lünenschloss, 1998). Kenis *et al.* (2000) defined *P–T* conditions of a progressive deformation process at the northern Variscan front (northern France) by studying distinct vein generations, pre-Variscan ($\leq 310\,^{\circ}$C), Variscan (260–200 °C) and post-Variscan (50–85 °C). Other investigations worldwide have been carried out on different deformation-enhanced syntectonic fluid systems (Xu, 1997; Muchez & Sintubin, 1998; Costagliola *et al.* 1999; Evans & Battles, 1999; O'Reilly & Parnell, 1999; Renard, Gratier & Jamtveit, 2000; Bons, 2001; Srivastava & Sahay, 2003).

The aim of this study is to determine the characteristics of the Variscan fluids and their migration during burial and deformation of Devonian and Lower Carboniferous calcareous rocks in the Moravian Karst area, Czech Republic (Figs 1, 2). Using a combination of petrography, cathodoluminescence, geochemistry, stable isotope and microthermometry techniques, syntectonic veins developed in a thin pile of calcareous strata above an old and very stable Proterozoic basement (Brunovistulian terrane: Dudek, 1980; Brochwicz-Lewinski *et al.* 1986) have been studied. There are presently few constraints on the *P–T* conditions during Variscan tectonics in the Moravian Karst and this study contributes to a better understanding of the Variscan tectonics and models of fluid flow of the eastern border of the Bohemian Massif.

2. Methodology

Syntectonic veins have been studied from several quarries in different parts of the Moravian Karst. These large exposures allowed syntectonic Variscan veins to be distinguished from younger vein generations (post-Variscan: Slobodník, Muchez & Viaene, 1997) and study of their structural context within the folded strata to be determined. Calcite veins were sampled for a detailed petrographic study with incident and transmitted light and cathodoluminescence (CL). Cathodoluminescence microscopy has been applied to distinguish multiple vein generations (Kappler & Zeeh, 2000; Ferket *et al.* 2003) or for a better interpretation of recrystallization or alteration of wall rock (Hilgers & Urai, 2002). Luminescence characteristics, with respect to CL-theory (e.g. Yardley & Lloyd, 1989; Pagel *et al.* 2000), of host rock and veins can indicate a geochemical equilibrium between fluid and rock and will allow a better interpretation of stable isotope data. Based on this petrographic investigation, samples were selected for a microthermometric analyses of fluid inclusions and for a geochemical and stable isotopic analyses of the vein calcites. The results obtained during this investigation were compared with those of other methods applied in the Moravian Karst area (e.g. illite crystallinity, vitrinite reflectance R_r: Franců, Franců & Kalvoda, 1999).

Aliquots (3 g) from calcite sampled from the syntectonic veins were analysed for CL-controling elements employing standard atomic absorption spectrometry (for Mn) and photometric (for Fe) analytical methods with precision better than 0.05 %.

Thermometric analyses have been carried out on a Linkam heating–freezing stage, and synthetic fluid inclusions (SynFlinc) were used for calibration. The homogenization temperature of the fluid inclusions (T_h), the temperature of first melting (T_{fm}) and the temperature of the final melting of ice (T_m) were measured during heating and freezing runs on doubly polished samples.

The carbon and oxygen isotopic composition of the vein calcites and their carbonate host-rock were analysed on a Finnigan-Mat Delta-E mass spectrometer (corrections after Craig, 1957) with the reproducibility better than 0.05 ‰ for oxygen and carbon (1σ, N = 4). Analyses were performed at the Free University of Brussels and at the Geological Survey in Prague

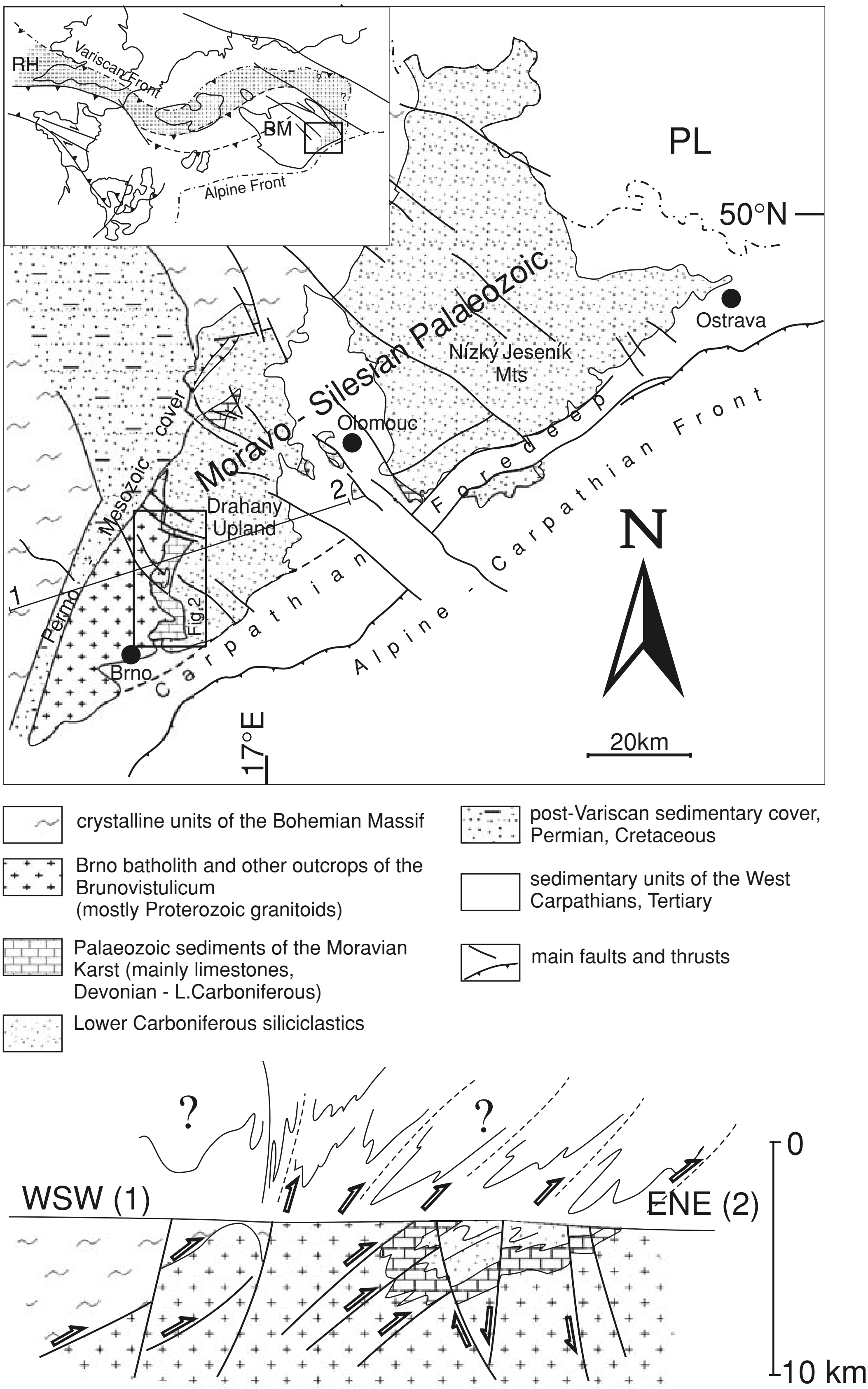

Figure 1. Schematic geological map of the eastern part of the Bohemian Massif and the cross-section (1–2) of the area of interest. Location box for Figure 2 indicated. Inset map: position of the Bohemian Massif (BM) in the Variscan belt and in Rhenohercynicum (RH) (modified after Franke, Dallmeyer & Weber, 1995). The cross-section with an indication of geological structures above recent erosion surface is modified after Hladil *et al.* (1999) without Permian and younger sedimentary cover.

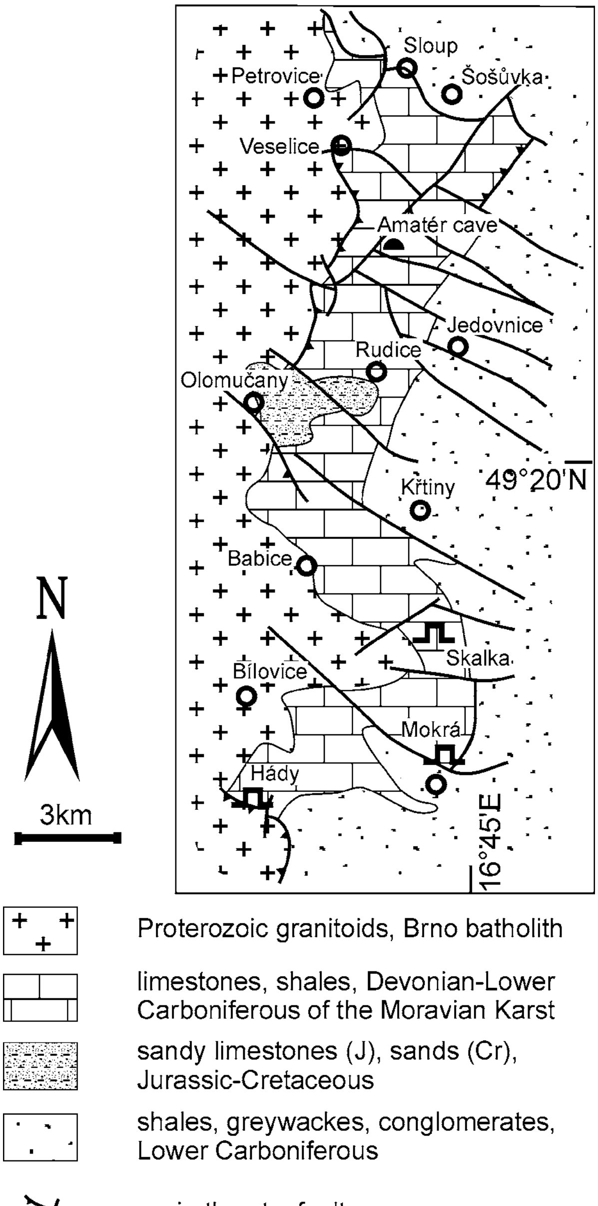

Figure 2. Schematic geological map of the Moravian Karst (modified after Dvořák & Pták, 1963; Hanžl *et al.* 1999).

(analyst J. Hladíková). Both laboratories use the same analytical procedure and internal standards. All values are reported in per mil relative to Vienna-Pee Dee belemnite (V-PDB) by assigning a δ^{13}C value of 1.95 per mil and a δ^{18}O value of −2.20 per mil to NBS 19 (NIST, Gaithersburg, USA).

Six samples of vein calcites, carbonate host-rock and siliciclastics have been analysed to determine the ^{87}Sr/^{86}Sr ratio. For the Sr-isotope analysis, 1 g of homogenized sample was dissolved in 3M acetic acid to avoid dissolution of silicate inclusions with potentially increased Rb contents. The obtained solution was purified, decanted and centrifuged to remove insoluble residuum. Pure solution was evaporated to dryness, poured with 6M hydrochloric acid (HCl), again evaporated to dryness and dissolved in 1 ml of 2.5M HCl. Strontium was separated by elution chromatography using quartz glass columns filled with 10 cm^3 of a Dovex Biorad 50 × 8 ion exchanger with grain size between 200 and 400 mesh. Supra-pure grade chemicals together with deionized water (18.3 $\mu\Omega$) were used for sample preparation. Total analytical blank was lower than 2 ng. Measurements were performed using a VG54E mass spectrometer at the Polish Academy of Science, Warsaw, Poland. Presence of ^{85}Rb was checked during the measurements. The 85/86 mass ratio was lower than 0.001 in all measured samples. The international standard SRM 987 with the accepted ^{87}Sr/^{86}Sr value of 0.710248 was measured together with the samples and all results were corrected to this value. The standard deviation (1σ) for a single measurement was better than 2 × 10^{-5}.

3. Geology of the area

3.a. Lithostratigraphy

The Moravian Karst consists of Devonian and Carboniferous strata that belong to the Moravo-Silesian Palaeozoic unit (MSP; Figs 1, 2), forming part of the Rhenohercynian zone (Franke, Dallmeyer & Weber, 1995). Two main lithostratigraphic units of Palaeozoic age can be distinguished in the Moravian Karst: the Macocha and Líšeň formations (Fig. 3). The basement in the area is composed of magmatic (580–590 Ma: Van Breemen *et al.* 1982; Finger *et al.* 2000) and metamorphic rocks of Proterozoic age, termed Brunovistulicum (Dudek, 1980). This basement crops out in the Brno batholith that dominantly contains granitoid rocks and borders the Moravian Karst area to the west. The sedimentary sequence above the basement begins with a basal Devonian conglomerate (Fig. 3). The overlying Macocha Formation represents Givetian (Lažánky Limestone) and Frasnian (Vilémovice Limestone) shallow water sedimentation on a carbonate platform; these limestones are very pure and are massive in character (Dvořák & Pták, 1963, Hladil *et al.* 1991). The limestones of the younger Líšeň Formation (Famennian to Tournaisian) are often clay-rich, reflecting a deepening of the depositional environment (Dvořák, 1990). The thin-bedded Hády-Říčka Limestone with intercalations of shales and the Křtiny Limestone with typical nodular structure are the two principal members of the Líšeň Formation (Fig. 3). The succeeding siliciclastics of the Lower Viséan are typical of flysch sedimentation. The lower part of this flysch sequence consists of shales of the Březina Formation, followed by the silty shales and fine-grained greywackes of the Rozstání Formation. The Palaeozoic sedimentary sequence ends with shales and conglomerates of the Myslejovice Formation of Late Viséan age.

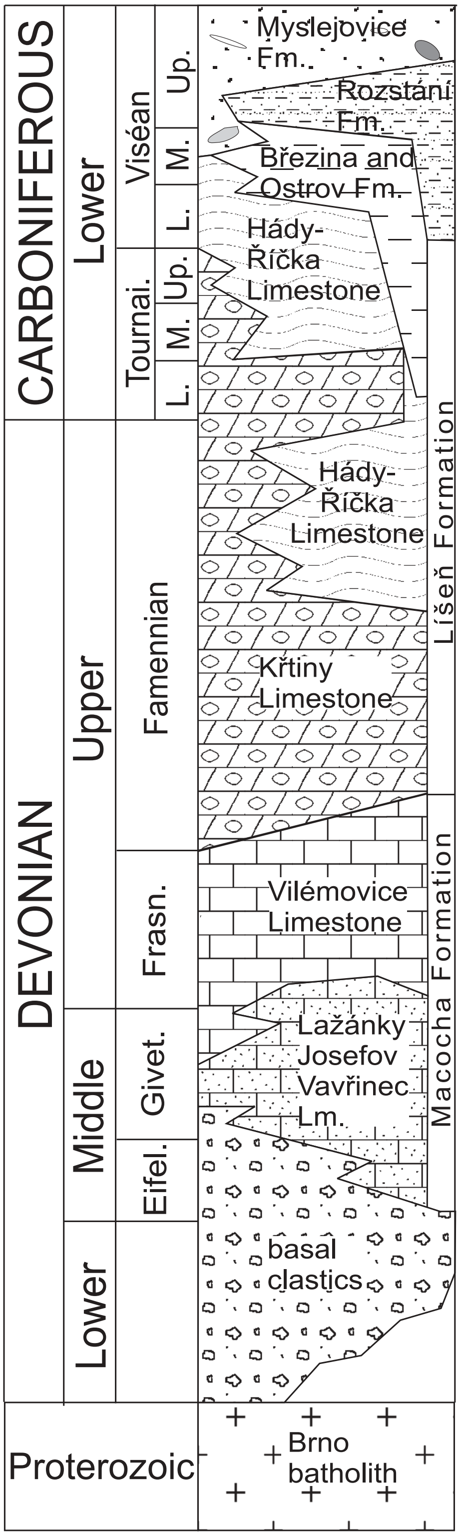

Figure 3. Lithostratigraphic column of the Moravian Karst area (compiled and modified after J. Dvořák *in* Musil, 1993).

3.b. Tectonics

The Moravian Karst is underlain and bordered by Proterozoic granitoids on the west, and on the north, east and south plunges under Carboniferous siliciclastics and Tertiary sediments, respectively (Figs 1, 2). The Moravian Karst area originally formed a large Givetian–Frasnian platform that belonged to the extensive network of carbonate platforms which rimmed the northern coasts of the Rhenish basins from SW England to Moravia (Hladil *et al.* 1999). The Variscan convergence is linked with closure of the Rhenohercynian ocean in Late Devonian–Early Carboniferous times. Shortening of the sedimentary sequence predates folding and was more intense towards the NNE from the investigated area (e.g. Hrouda, 1981). During ductile deformation and cleavage development, water from dewatering of clay minerals was an important agent of metamorphism (Dvořák, 1989). Subsequently, the Moravian Karst area became a part of the Moravo-Silesian Shear Zone (Rajlich, 1987; Schulmann *et al.* 1991; Fritz & Neubauer, 1993; Grygar & Vavro, 1994), which is a main structure in the region stretching NNE–SSW along the east border of the Bohemian Massif. This zone developed during the Late Carboniferous (Rajlich, 1987; 1990) and is up to 50 km wide, involving the Moravo-Silesian Palaeozoic and adjacent crystalline units to the west. Due to major dextral movement in the zone, a complicated system of folds and thrusts occurred. The period of folding, thrusting and rotation culminated in superimposed northwards nappe transport and stacking (Hladil, 1991; Grygar & Vavro, 1994; Krs *et al.* 1995; Tait, Bachtadse & Soffel, 1996; Orel, 1996). The Moravian Karst includes northwesterly oriented Namurian thrusts with dextral horizontal shear (Hladil *et al.* 1991; Melichar & Kalvoda, 1997), which were recognized by Kettner (1942) more than 60 years ago. The heat flow gradually increased and therefore the peak metamorphism was reached in many places after folding (Dvořák, 1989). Crustal thickening was followed by crustal extension and gravitational collapse (Rajlich, Slobodník & Novotný, 1989; Zulauf *et al.* 1997), and elevated heat flow (Dallmeyer, Franke & Weber, 1995). This extension was associated with faulting which made possible the convection of hot fluids for a very long time, resulting in intensive heat flow (Dvořák, 1989).

In the northeastern part of the Moravo-Silesian Palaeozoic, the maximum coal rank in the Bohemian Massif was found (Dvořák & Skoček, 1975). Increased heat flow had already taken place during the Carboniferous, essentially affecting the coalification of organic matter in the Carboniferous sediments (e.g. a palaeo-geothermal gradient between 70 and 90 °C has been discussed for late Carboniferous times in the northeastern part of the Moravo-Silesian Palaeozoic, as in the foreland: Dvořák *et al.* 1997). Higher heat flow and existence of magma sources in the crust is indicated by the Upper Carboniferous (Stephanian) lamprophyric dykes widespread in the region (Dvořák & Přichystal, 1982). An increasing temperature in a NNW direction across the region is in good agreement with the maximum deformation recorded in this section of the Moravo-Silesian Palaeozoic unit (Grygar & Vavro, 1994).

Evidence for a NNW increase of the palaeotemperature field in the Drahany Upland (western part of the Moravo-Silesian Palaeozoic unit) is provided by the vitrinite reflectance (R_r) and illite crystallinity data (Franců, Franců & Kalvoda, 1999). Temperature differences within the Moravian Karst were small and the illite crystallinity and vitrinite reflectance were 0.64 and 1.38–1.57 % respectively. In the south (Mokrá area), the maximum palaeotemperature was between 130 and 170 °C (Franců *et al.* 1998; Franců, Franců & Kalvoda, 1999). In the northern part of the Drahany Upland, the maximum was between 170 and 200 °C. Except for the high geothermal gradient values (up to 200 °C km^{-1}: Dvořák 1989) found to the west of the Drahany Upland, more exact modelling of heat flow has been applied in the area, based on a few boreholes (Franců *et al.* 2002). Palaeo-gradients between 27 and 58 °C km^{-1} (between 0–4 km) match the observed metamorphism and burial alternative models more closely.

Development of the area during Mesozoic and Tertiary times took place within a platform regime and under the influence of West Carpathian tectonic events. It is believed that there was no gradual development of tectonic structures from the Variscan into post-Variscan period. The post-Variscan types of hydrothermal veins in the region have fairly different genetic conditions (e.g. Malkovský, 1978; Slobodník, Muchez & Viaene, 1997) and are out of the scope of this paper.

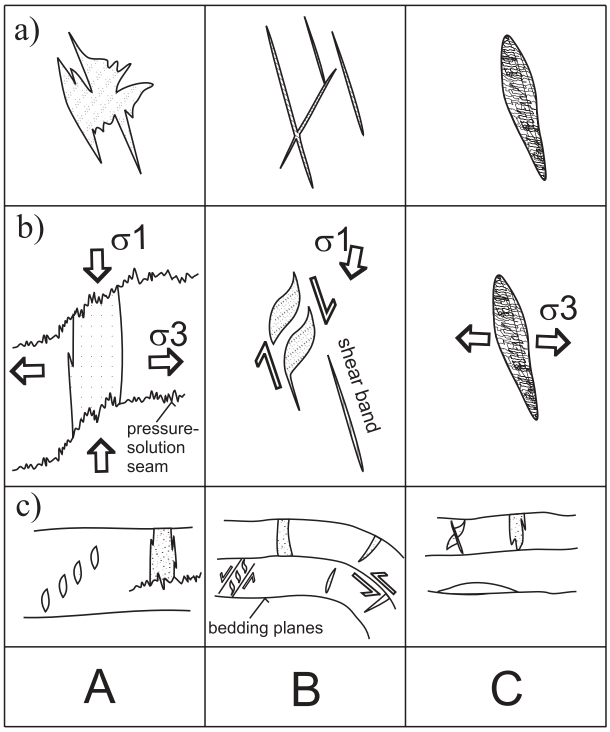

Figure 4. Example schemes of main structural features of the classified calcite veins (A, B, C): (a) the most common shape of veins; (b) typical vein geometry with respect to the stress fields; (c) position and orientation of veins in sedimentary beds.

4. Structural and petrographic characteristics of the Variscan veins

Variscan veins have been divided into three groups, based on their structural and petrographic properties (Fig. 4). All veins are calcite-filled and show several features of deformation such as recrystallization, an undulatory extinction and curved twin lamellae. Milky calcites with fine- and medium-grained crystals are most abundant in the veins of group A and B and light rose medium-grained calcite is common for group C.

Veins of group A include strongly deformed calcites that are omnipresent in massive Frasnian limestones. They often form very irregular veins or complicated sigmoidal veins arranged into arrays (Figs 4, 5a, b). The length of veins is usually 20–40 cm at most, and thickness is highly variable but mostly between less than 1 cm and several centimetres. The simple veins show a lenticular shape and have formed as tension gashes with a clear relationship to pressure-solution seams (Fig. 4). Subsequent shearing of these veins caused deformation of the calcite cement, followed by recrystallization, and hence their internal structure is blocky, fine-grained and/or with different sizes of grains. Under the microscope, calcites are cloudy and contain a large amount of tiny (< 1 μm) fluid inclusions (FIs). The omnipresence of these fluid inclusions is responsible for the milky-white hue of the hand specimens. They represent a closed space from the structural point of view, but there are no microstructures (selvage) indicating the dominant mass transport mode into the fractures (Oliver & Bons, 2001). However, vein calcites show roughly the same luminescence colour and intensity as their host limestone (cf. Van Geet *et al.* 2002), that is, a dull yellow-brown hue for both, suggesting a chemical identity at least for CL-activating elements including REE (Canole, Odonne & Polve, 1997).

Group B veins are mostly regular and straight, occuring in both massive Frasnian and bedded Famennian limestones. They cross-cut the veins of group A. The length of the veins is greater than that of the A veins and is between several centimetres and tens of centimetres but they are thinner (from < 1 mm up to 4 cm), developed from shear fractures in the compressional field. There are many indications that veins of group B have been formed mainly during folding and shearing of rocks. They are very frequent in the well-bedded and intensely folded Famennian limestones. Veins show a clear relationship to the fold geometry (ac- or bc-positions) and they are oriented normal to the extensional stress (e.g. Fig. 6c, d). Other regular calcite veins developed perpendicularly to the bedding planes and formed due to interlayer-slip that gave rise to in-filling tension structures, dilational jogs (Fig. 4c). The curved shapes of both B and A veins

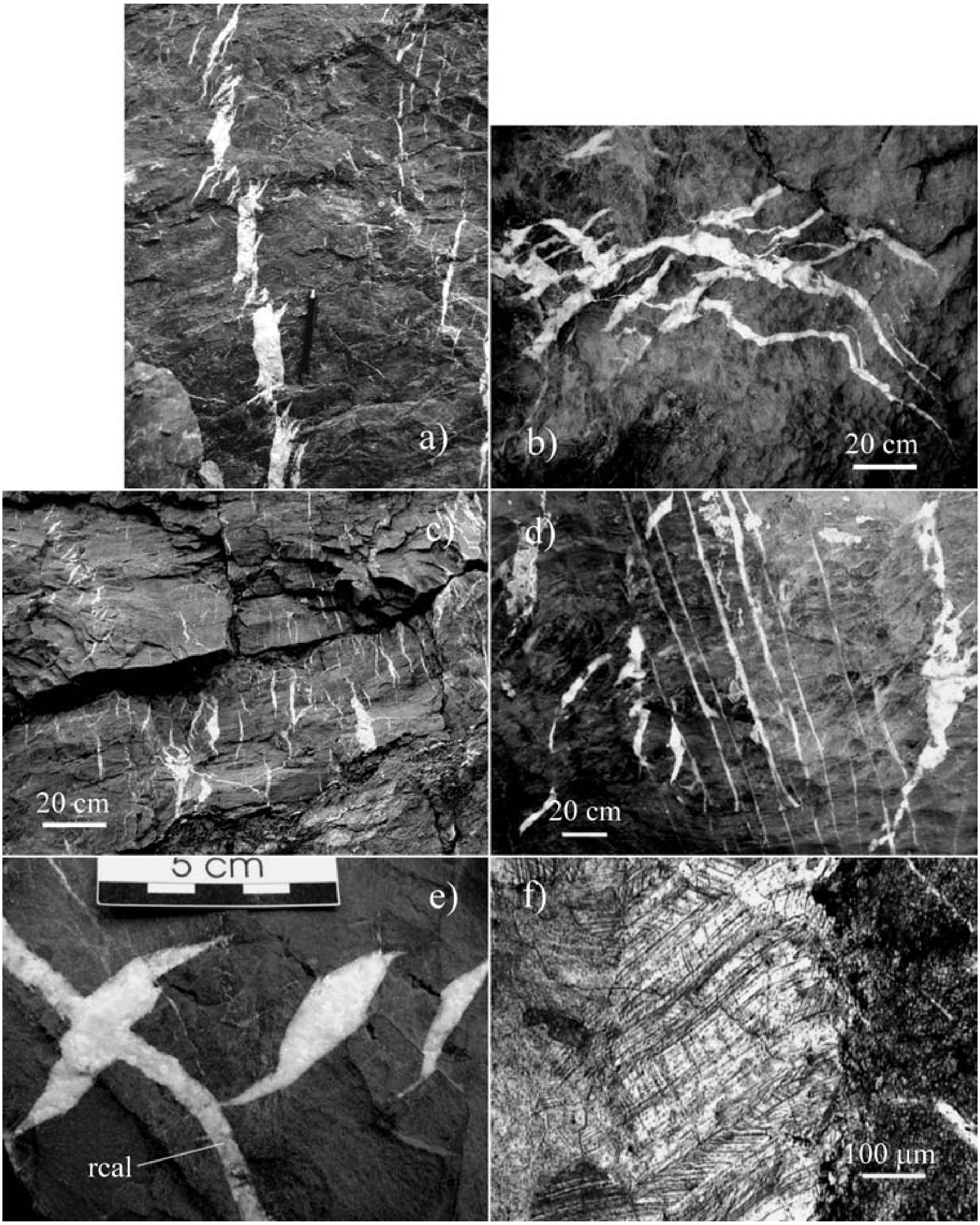

Figure 5. (a) Irregular an echelon white calcite veins (A group), Frasnian limestone, Sloup, Moravian Karst; (b) irregular white calcite veins (A group), Frasnian limestone, Sloup, Moravian Karst; (c) calcite veins (B group) perpendicular to bedding planes in massive Frasnian limestone, Mokrá, Moravian Karst; (d) irregular (A group) and regular white calcite veins (B group), Frasnian limestone, Sloup, Moravian Karst; (e) sigmoidal lenticular white calcite veins in array cross-cut by the straight, regular vein with rose calcite (rcal, C group), Líšeň, Moravian Karst; (f) syntectonic fibrous calcite vein, Famennian limestone, Líšeň, Moravian Karst.

(Fig. 5b, d, e) suggest a brittle–ductile failure mode during precipitation of the veins.

Veins in some places form a very regular and dense network, often including conjugate systems (Fig. 6). The acute bisector of the vein arrays in the massive Frasnian limestone is usually either subnormal to the bedding and to stylolite seams or parallel with bedding (Fig. 6d). This suggests the genetic link of these

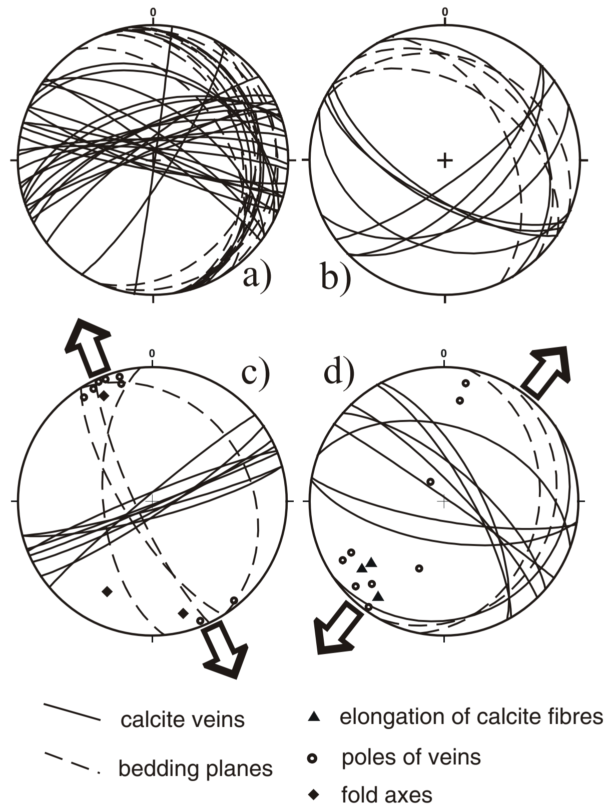

Figure 6. Geometry of Variscan syntectonic calcite veins. (a) Calcite veins B, Mokrá – western quarry; (b) conjugate calcite veins B, Skalka quarry; (c) white veins B associated with a fold geometry, Hády, (d) rose calcite veins C, Hády.

Table 1. MnO and FeO content and MnO/FeO ratio of calcites from the Moravian Karst

Sample	FeO (wt %)	MnO (wt %)	MnO/ FeO	Classification of veins (A, B, C)
MW5 A	0.35	0.00	0.00	A, Variscan
MW5 B	0.52	0.00	0.00	A, Variscan
M2	0.34	0.00	0.00	A, Variscan
MW5 C1	0.31	0.00	0.00	B, Variscan
MS2	0.20	0.00	0.00	B, Variscan
M37	0.20	0.00	0.00	B, Variscan
HL39	0.25	0.04	0.16	B, Variscan
A4	0.07	0.04	0.57	B, Variscan
SZ24	0.03	0.005	0.17	B, Variscan
SZ27	0.17	0.008	0.05	B, Variscan
M38	0.32	0.03	0.09	C, Variscan
HL46	0.29	0.03	0.10	C, Variscan
HL36	0.29	0.03	0.10	C, Variscan
S3	0.09	0.01	0.11	C, Variscan
S4	0.11	0.01	0.09	C, Variscan
S5a	0.06	0.02	0.33	C, Variscan
SZ16	0.01	0.01	1.00	C, Variscan
A6	0.02	0.02	1.00	Post-Variscan
A6a	0.01	0.01	1.00	Post-Variscan
A6b	0.05	0.02	0.40	Post-Variscan
A2	0.22	0.10	0.45	Post-Variscan
A6ab	0.25	0.36	1.44	Post-Variscan
MV3	0.22	0.21	0.95	Post-Variscan
M10	0.23	0.20	0.87	Post-Variscan
HL51	0.38	0.15	0.39	Post-Variscan
S5	0.08	0.07	0.88	Post-Variscan

Sample localities: M – Mokrá, HL – Hády, S – Skalka, A – Amatér cave.

veins with a maximal local principal stress. Increased pressure plays an important role in dissolving rock-forming minerals (carbonates) and redistribution of fluid into open fractures.

The vein characteristics mentioned above are common in many fold-and-thrust belts (e.g. Dunne, 1986) and have been recently well described by Micarelli *et al.* (2005).

Veins in tension gashes show a fibrous structure (Fig. 5), characteristic of a crack-seal origin (Ramsay, 1980). There are several types of microstructures important for understanding the veining mechanism. Curved fibre crystals with growth surface and selvage present at one side of the wall point to shearing during growth of grains (Fig. 7a), while calcite in other veins shows a recrystallized equal-grained structure (Fig. 7b). Insoluble residuum forming selvage on the vein walls (Fig. 7a, b), frequently present in this type of vein, suggests a diffusional mechanism of mass transfer from the wall rock (Oliver & Bons, 2001). Multiple reopening of fractures is well documented by bands of rock inclusions along vein walls (Fig. 7c).

The less deformed veins of group C often have a light rose colour and, according to cross-cut relationships, they are younger than the veins of group B (Fig. 5e). Their structural characteristics are similar to the veins of group B but they are generally less abundant. Veins of group C are, however, more abundant in well-bedded Famennian strata, where they developed as lenticular veins. Veins of group C are up to 15 cm thick with no indication of wall-rock alteration. Blocky or stretched crystal structures are abundant (Fig. 7d) and those veins are normal to the extensional stress as lenticular gashes (Figs 4, 6d). Stretched crystal veins are of the crack-seal type and crystals have a roughly constant width across the vein. Sealing sites cannot be distinguished because they are distributed through the stretching grains (Ramsay, 1980; Oliver & Bons, 2001). All structural features of this type of vein suggest fairly pure extensional regimes during their formation within brittle failure mode (e.g. Sibson, 2000). Cathodoluminescence analyses of these veins show a more intense yellow-brown to brown luminescence than the host-rock, and some grains and parts of veins can be slightly zoned. Different luminescence of veins and wall rock suggests a different content of CL-activation elements (e.g. Budd, Hammes & Ward, 2000) and hence possibly modest chemical fluid/rock disequilibrium.

5. Geochemistry

The dull luminescent syntectonic calcites have a low Mn content and a low Mn/Fe ratio (Table 1). This relationship between the Mn and Fe content of calcites and their luminescence has been described elsewhere (e.g. Barnaby & Rimstidt, 1989).

The $^{87}Sr/^{86}Sr$ values of the white vein calcites of groups A and B are comparable to those of

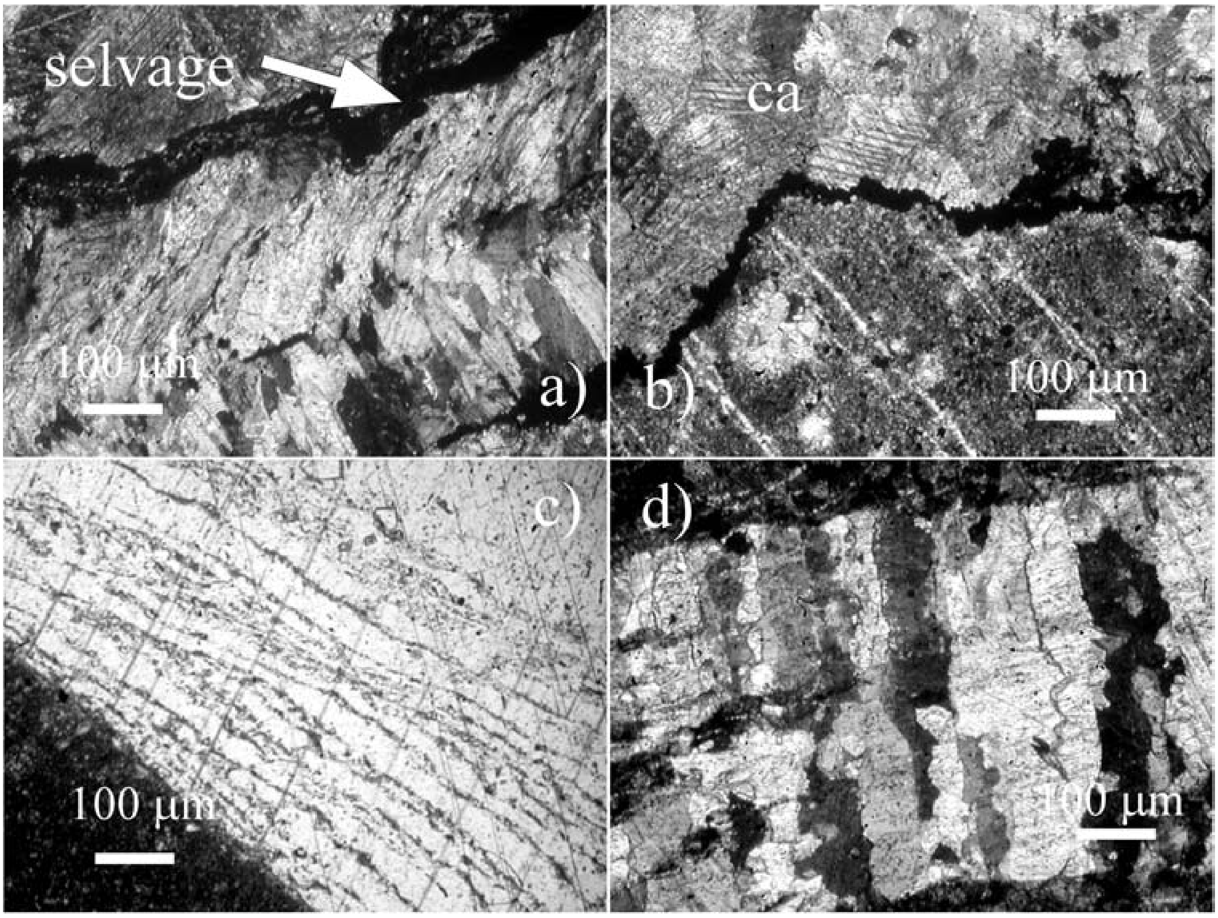

Figure 7. (a) Fibrous vein with white calcite and selvage on the wall, crossed polars; (b) selvage between rock and white vein calcite (ca) with an equal-grained structure, crossed polars; (c) bands of rock inclusions along wall of calcite vein, parallel polars; (d) stretched crystal structure of rose calcite vein (C), crossed polars.

the Devonian carbonate host-rock and range between 0.7078 and 0.7082 (Tables 2, 3). The strontium isotopic composition of the rose calcites of group C is distinctly more radiogenic (0.7086). The carbon isotopic composition of both vein calcites and the host limestones is similar: δ^{13}C values of the limestones and the white calcites are from -0.7 to $+2.6$ and between $+0.1$ and $+2.5$ ‰ V-PDB, respectively. The δ^{13}C values of the rose calcites are between -0.3 and $+1.6$ ‰ V-PDB. The δ^{18}O values show a large spread and are between $+14.8$ and $+26.1$ ‰ SMOW (Tables 2, 3). Analyses of the limestones range between $+20.9$ and $+26.8$, of the white calcites between $+17.7$ and $+26.1$ and of the rose calcites between $+14.8$ and $+20.7$ ‰ SMOW. There is a large overlap in the oxygen isotopic compositions of the white calcite veins and their host rock, but the younger generation of rose calcites have distinctly lower δ^{18}O values (Fig. 8a). A shift towards lower δ^{18}O values was observed in one vein (group B of white calcite veins) from the older calcite adjacent to the wall of the vein (no. 1 in Fig. 8a) to the central younger part (no. 2 in Fig. 8a). This trend is consistent with lower δ^{18}O values in younger rose calcites (group C).

Since the stable isotopic composition of the white calcites falls mostly within the range of the surrounding limestones, the ambient fluid from which the calcites precipitated was likely isotopically buffered by this host-rock (e.g. Gray, Gregory & Durney, 1991). The similar strontium isotopic signature of the white calcites and the limestones also indicates a buffering of the strontium isotopic composition of the fluids by the host-rock.

The rose calcites generally have a different stable isotopic composition from the white calcite cements. In addition to depletion in ^{18}O, the higher strontium isotopic composition of the rose calcites demonstrates that the younger mineralizing fluids were no longer in isotopic equilibrium with the host rock. Assuming frequent occurrence of the rose calcite veins in well-deformed, fractured and folded, bedded limestones, this means that their parent fluids migrated through the rocks with increased permeability. The greater thickness of the veins and their more frequent occurrence along bedding planes suggest that a greater amount of fluids could flow through the rocks. In light of these indications, it is likely that the precipitation of the rose calcites took place in

Table 2. Carbon, oxygen and strontium isotopic composition of Variscan syntectonic vein calcites

Sample	δ^{18}O SMOW	δ^{13}C VPDB	^{87}Sr/^{86}Sr	Classification of veins (A, B, C) and notes
H60a	20.807	0.200	0.707789	A, white calcite in Famennian
H60	17.508	0.600		A, white calcite in Famennian
A1	24.162	1.440	0.708011	A, white calcite in Frasnian
M24a	23.725	0.080		A, white calcite in Frasnian
M-W5	22.952	0.651		A, white calcite in Frasnian
M1	25.158	0.310		A, white calcite in Frasnian
M2	25.199	0.140		A, white calcite in Frasnian
HL 53	17.681	1.787		B, white calcite in Famennian
HL 53	20.894	1.924		B, white calcite in Famennian
HL 37	26.065	2.392		B, white calcite in Famennian
HL 38	24.149	2.467		B, white calcite in Famennian
HL 39	24.672	2.477	0.708243	B, white calcite in Famennian
HL 52	25.717	2.589		B, white calcite in Famennian
A9	21.056	−1.488		B, white calcite in Frasnian
A7	21.846	−1.747		B, white calcite in Frasnian
M 39	24.182	1.116		B, white calcite in Frasnian
M 40	24.716	1.262		B, white calcite in Frasnian
HL 36	19.852	0.624		C, rose calcite in Famennian
HL 44	19.985	0.626		C, rose calcite in Famennian
HL 47	19.376	0.486		C, rose calcite in Famennian
HL 48	19.204	0.361	0.70863	C, rose calcite in Famennian
HL 41	18.963	0.930		C, rose calcite in Famennian
HL 43	18.662	0.506		C, rose calcite in Famennian
HL 46	18.425	−0.084		C, rose calcite in Famennian
HL 49	18.190	0.568		C, rose calcite in Famennian
HL 51	17.806	0.385		C, rose calcite in Famennian
HL 50	17.445	0.780		C, rose calcite in Famennian
H31	16931	0.190		C, rose calcite in Famennian
H32	17.199	1.410		C, rose calcite in Famennian
M5	15.900	0.450		C, rose calcite in Frasnian
M 38	15014	0.917		C, rose calcite in Frasnian
M-V3	15.267	0.795		C, rose calcite in Frasnian
M-W1	14842	1.564		C, rose calcite in Frasnian
M-W3	15.871	0.852		C, rose calcite in Frasnian
M4	20.704	0.290		C, rose calcite in Frasnian
M 33	18.521	−0.314		C, rose calcite in Frasnian
S4	19.117	0.334		C, rose calcite in Frasnian

Sample localities: HL, H – Hády, A – Amatér cave, M – Mokrá, S – Skalka.

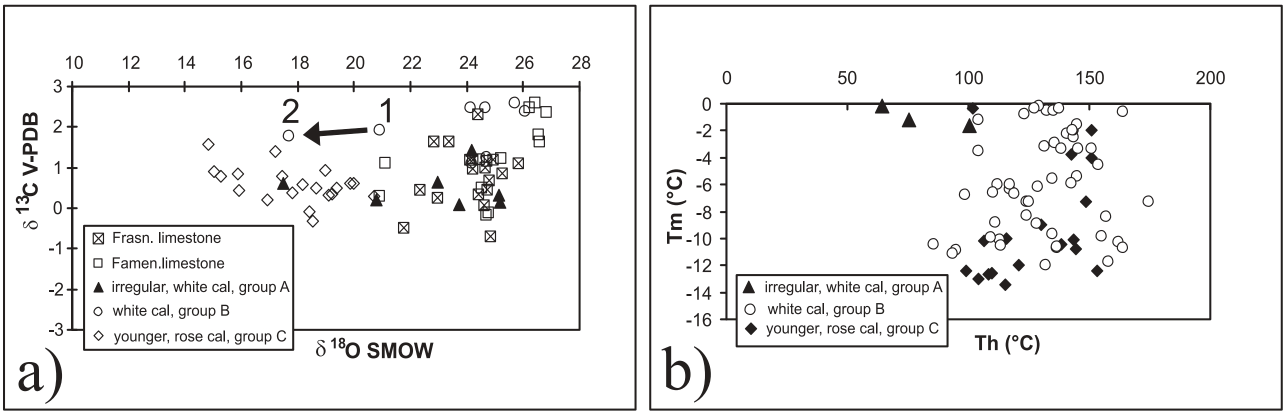

Figure 8. (a) δ^{18}O–δ^{13}C plot showing the isotopic compositions of syntectonic calcites (cal) and of the host-limestones; (b) plot of the homogenization temperature versus the temperature of the final melting of ice in fluid inclusions in syntectonic Variscan calcites, Moravian Karst.

a geochemically more open system than the white calcites.

6. Microthermometry

One- and two-phase aqueous fluid inclusions (FIs) occur in the white and rose calcite cements. The one-phase FIs are mostly small (*c.* 2 μm or less), more or less randomly distributed and of uncertain origin. Two-phase FIs present in growth zones (primary fluid inclusions) were carefully selected for this microthermometric study. In addition, only calcite crystals with no or only minor indications of deformation were used to avoid stretched or re-equilibrated fluid inclusions

Table 3. Carbon, oxygen and strontium isotopic composition of rock samples

Sample	$\delta^{18}O$ SMOW	$\delta^{13}C$ VPDB	$^{87}Sr/^{86}Sr$	Notes
HL 39r	26.245	2.462		Rock, Famennian
HL 38r	26.432	2.604		Rock, Famennian
H34r	26.590	1.620		Rock, Famennian
HL-1r4	26.819	2.346		Rock, Famennian
HL-1r5	26.536	1.816		Rock, Famennian
HL-0r1	25.237	1.211		Rock, Famennian–L.Tournaisian
HL-0r2	24.771	−0.105		Rock, Famennian–L.Tournaisian
HL-0r3	24.555	0.507		Rock, Famennian–L.Tournaisian
HL 36r	24.459	1.194		Rock, Famennian–L.Tournaisian
HL 46r	24.679	−0.164		Rock, Famennian–L.Tournaisian
H60ar	20.910	0.300		Rock, Famennian–L.Tournaisian
H60r	21.116	1.100		Rock, Famennian–L.Tournaisian
M24r	24.611	0.060		Rock, Frasnian
M36r	24.663	1.220		Rock, Frasnian
Mr 1	24.756	0.425		Rock, Frasnian
Mr 2	25.263	0.851		Rock, Frasnian
Mr 3	24.711	1.233		Rock, Frasnian
Mr 4	24.953	1.185		Rock, Frasnian
Mr 5	24.312	1.163		Rock, Frasnian
Mr 6	24.363	1.163		Rock, Frasnian
Mr 7	24.410	0.326		Rock, Frasnian
Mr 8	24.878	−0.710		Rock, Frasnian
M-W5r	24.243	0.987	0.708206	Rock, Frasnian
M-W1r	22.840	1.619		Rock, Frasnian
M 39r	24.674	0.982		Rock, Frasnian
S4r	24.797	0.660		Rock, Frasnian
S2r	22.407	0.438		Rock, Frasnian
S7r	25.987	1.121		Rock, Frasnian
S8r	24.365	2.298		Rock, Frasnian
A1r	21.751	−0.491		Rock, Frasnian
A9r	22.992	0.254		Rock, Frasnian
A4ar	23.398	1.635		Rock, Frasnian
Hr-r			0.712657	Bulk rock sample: greywacke, conglomerate, shale, Lower Carboniferous

Sample localities: HL, H – Hády, A – Amatér cave, M – Mokrá, S – Skalka, Hr – Hrabůvka.

(see also Goldstein, 1986; Prezbindowski & Larese, 1987). Approximately 160 fluid inclusions between 3 and 15 μm were investigated.

The T_h values of both the white and rose calcites are between 64 and 174 °C (Fig. 8b). Several fluid inclusions in the white calcites have a first melting temperature around −21 °C, indicative of the H_2O–NaCl system. In most white calcites and in all rose calcites, T_{fm} values, however, are below −21 °C (up to −39 °C), suggesting that a more complex fluid system was trapped (e.g. Borisenko, 1977; Spencer, Møller & Weare, 1990). The range in T_m values is similar for the fluid inclusions in the white and rose cements, that is, between −0.2 and −14 °C (Fig. 8b). However, T_m values in the rose calcites are often the lowest measured and mostly below −8 °C. This range corresponds to a salinity of 0.35 to 17.25 eq. wt % NaCl (Bodnar, 1993).

7. Pressure and temperature conditions during vein formation

Trapping temperature (T_t), that is, the temperature during which the fluids were enclosed in the crystals and for primary inclusions the precipitation temperature of the crystals, can be calculated from the homogenization temperature by applying a pressure correction. Two isochores have been calculated; the first represents the A group of veins and second one B and C, which have similar microthermometric data. Both isochores have been calculated using the equations of Zhang & Frantz (1987) and a computer programme (R. J. Bakker, unpub. thesis, Univ. Heidelberg, 1999). Assuming hydrostatic and lithostatic pressure conditions, thermobaric gradients have been constructed for a geothermal gradient of 46 °C km^{-1} (Fig. 9). This geothermal palaeo-gradient is based on the work of Střelcová, Franců & Poelchau (1997), who investigated the temperature history of the Palaeozoic rocks in the area of the Drahany Upland, and the gradient has been modelled as rather lower for Namurian times. Undoubtedly the gradient could have changed during development of the veins and could have become progressively more likely to reach the higher values in the modelled range of 27–58 °C km^{-1} (Franců *et al.* 2002). Unfortunately it is not possible to use a definitive gradient value for each group of veins (A, B, C), since both isochores and thermobaric gradients constrain the P–T field during calcite precipitation. Lithostatic pressure conditions are between 180 and 1030 bar, corresponding to a depth of 0.7 to 3.8 km, considering 270 bar km^{-1} trapping temperatures are between 105 °C and 200 °C. The lower part of this range coincides with the temperature derived from the conodont alteration index (CAI). The CAI values are between 3.0 and 3.5 for the Famennian strata (determined by S. Helsen, pers. comm.) in the southern part of the Moravian Karst. These CAI values point to a maximum temperature of 120–150 °C. The vitrinite reflectance and illite crystallinity values of the Devonian and Lower Carboniferous strata in the Moravian Karst area and the surrounding Drahany Upland are between 1.38 and 1.57 % and between 0.32 and 0.55 Δ°2Θ, respectively (Franců *et al.* 1998; Franců, Franců & Kalvoda, 1999). Based on these parameters, the corresponding maximum temperature that affected the sediments was 130–170 °C.

Using the independent thermal indicators mentioned above (CAI, illite crystallinity), we may constrain the P–T conditions during the precipitation of the calcites. When assuming lithostatic conditions, the temperature range between 120 and 170 °C corresponds to a maximum ambient pressure between 580 and 880 bars (2.1–3.2 km) (Fig. 9). Considering the pure extension structures of C veins, mostly developed in seriously fractured rocks, and their isotopic and geochemical nature, the rose calcites are believed to be precipitated in an open fluid system. In this case, pressure conditions could be considered as fluctuating close to hydrostatic values (Sibson, 2000). Using the same thermal gradient of 46 °C km^{-1}, precipitating pressure conditions could be between approximately 300 and 500 bars, corresponding to a depth of 2.1 to 3.5 km.

8. Rock-buffered versus fluid-buffered system

Rock- and fluid-buffered veins represent two end-member models. In a rock-buffered model, the host rock determines the δ^{18}O composition of the fluid. In the second, fluid-buffered model, the geochemistry of the veins is buffered by a large reservoir of an aqueous fluid. Isotopic variations reflect a calcite–water system rather than a calcite–host rock fractionation. The distribution of data points along a zero fractionation line in the plot (Fig. 10a) of δ^{13}C values for calcite and host rocks (limestones) clearly reflects the same isotopic composition of carbon from vein calcites and of the host rock. This agreement suggests that the carbon in the vein calcites was derived from adjacent rocks. The same dependence can be observed also for the isotopic composition of oxygen in the A and B vein groups (Fig. 10b). A significantly different trend is shown by vein calcites from group C. The change in oxygen isotopic composition of vein calcites is remarkably variable, while that in host rocks is only

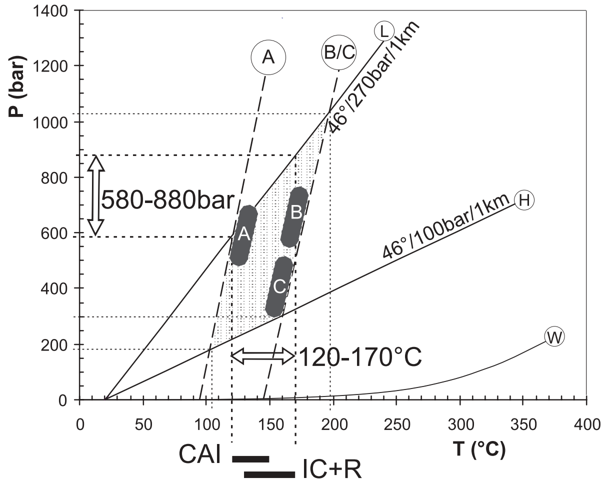

Figure 9. Pressure–temperature conditions of the precipitation Variscan syntectonic calcite veins in the Moravian Karst. Arrows indicate the most likely precipitation conditions (namely for white calcite veins) constrained by independent thermobarometers and P–T regions for particular vein groups (A, B, C). A, B/C – isochores representing calcite veins of group A and B+C groups, respectively, L, H – thermobaric lithostatic (L) and hydrostatic (H) gradients, W – two-phase equilibrium curve of the water system, CAI – temperature derived from the Conodont Alteration Index, IC + R – temperature derived from Illite Crystrallinity and Vitrinite Reflectance.

modestly so. This suggests the importance of another isotopic reservoir that contributed to oxygen isotopic composition of calcites C, as their trend is indicative of the fluid buffered system (Richards *et al.* 2002). Similarly there are two samples in the case of oxygen and one for carbon from the A vein group which fall outside the overall trend (Fig. 9a, b).

9. Discussion

Variscan tectonism led to an intense fracturing of the Palaeozoic rocks in the Moravian Karst and initiated fluid migration through the rock sequences. Syntectonic Variscan calcite veins in the area are abundant, confined and specifically related to Palaeozoic carbonates. Similarly, occasional tiny calcite veins in the basement and the Variscan generation of quartz veins in overlying Lower Carboniferous siliciclastics suggest a stratigraphically confined fluid system.

Three succesive generations/groups of calcite veins have been described in carbonate strata with relationships to developing tectonic structures during deformation of rocks. Veins in groups are, from the oldest A group to youngest C group, gradually less deformed, recrystallized and more regular in shape. Relative age is supported by cross-cut relationships. The relationship to solution structures such as stylolite seams is pronounced in many places, pointing to a derivation of the vein material from the host rocks during burial and deformation (Ramsay & Huber,

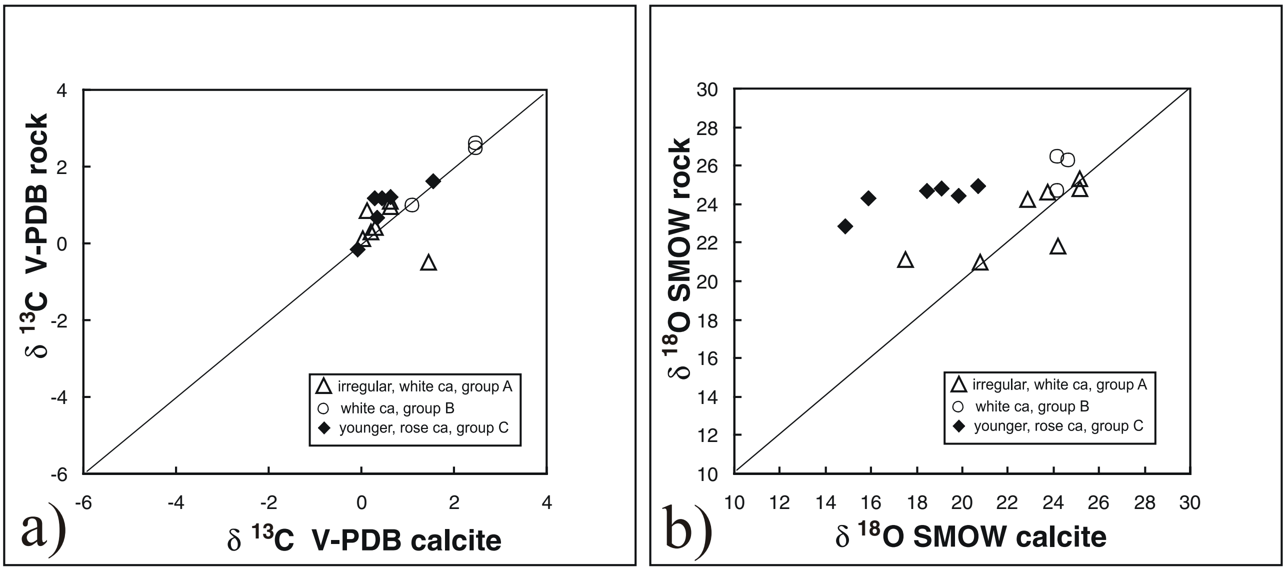

Figure 10. (a) Vein calcite δ^{13}C v. whole-rock (limestone) δ^{13}C values from the Moravian Karst; data points of three groups of the Late Variscan calcite veins (A, B, C) are distributed along zero fractionation line. (b) Vein calcite δ^{18}O v. whole-rock (limestone) δ^{18}O values from the Moravian Karst; data points are distributed close to a zero fractionation line or have a horizontal trend.

1987). Fibrous vein structures, often with curved fibres and selvages on vein walls, suggest a diffusion mass transport mechanism from the rock into veins during deformation. Multiple bands of rock inclusions along vein walls pointing to reopening events suggest a pressure-dependent closed system (Oliver & Bons, 2001). Similar features have been reported from quartz veins in siliciclastic terrains (Knoop, Kennedy & Dipple, 2002) and from carbonate veins in collisional belts with thick piles of sediments (e.g. Srivastava & Engelder, 1990; Kirschner & Kennedy, 2001). In most cases, the veins were precipitated in a closed system. Even in terrains with large thrust faults, only limited fluid flow occurred across faults and the system can be considered as semi-closed (Kirschner & Kennedy, 2001). Closed systems mostly operated when the volume of fluids was limited, expressed as $X_{rock} \rightarrow 1$ and defined as a rock-buffered system (e.g. Richards *et al.* 2002). Considering field observations of the investigated area, where calcite veins are mostly short and thin, the mole fraction of migrating fluids in the host-rock must have been low. Furthermore, restricted open fractures imply low permeability of the rocks mostly resulting from a transpressional/convergent regime producing ductile and brittle–ductile structures. These are associated with the veins A and B.

Similarly, rock buffering for white vein calcites A and B is supported by isotopic compositions of oxygen, carbon and strontium, which are strongly dependent on the rock composition (Figs 8a, 10, Tables 2, 3). This relationship reflects a very restricted distance of the fluid flow, confined to the proximity of the veins. Such bed-scale fluid migration was defined for veins in the Ouachita orogenic belt when diffusion was the main mechanism of material transfer (Richards *et al.* 2002). Stable isotope studies of syntectonic veins and their host rocks from the southeastern Canadian Cordillera also suggest that veins formed predominantly in a closed, rock-buffered system (Nesbitt & Muehlenbachs, 1989; 1997; Kirschner & Kennedy, 2001). The δ^{18}O and ^{87}Sr/^{86}Sr values of the rose calcite cements are, however, different from that of their host-rock. This reflects precipitation from fluids affected by another isotopic reservoir. The lower δ^{18}O (Figs 8a, 10b) and higher δ^{87}Sr/^{86}Sr values of the rose vein calcites are indicative of a more open system. Eppel & Abart (1997) noted that an open system within a deformational setting is related to structural and lithological discontinuities and occurs when isotopically distinct rock reservoirs are juxtaposed at a structural boundary. The most instructive example is the fluid flow along the Glarus thrust of the eastern Helvetic Alps, where several reservoirs contributed to the fluid flow system (Badertscher *et al.* 2002). Moreover, open systems are associated with higher permeabilities of the rocks (e.g. Gray, Gregory & Durney, 1991; Marquer & Burkhard, 1992; Losh, 1997), which is the case with the extensional regime of C veins. The higher ^{87}Sr/^{86}Sr ratio of the rose calcites compared with that of the white calcites suggests interaction of the fluids with a more enriched source. Such a radiogenic source is present laterally in the Lower Carboniferous siliciclastics (^{87}Sr/^{86}Sr ratio of an average bulk sample is 0.712657; Table 2) or in the underlying crystalline granitic basement (Finger *et al.* 2000; Kalvoda *et al.* 2002). The Sr-isotopic signature of the C veins requires migration of their parent fluids over greater distances than on a bed-scale, most likely by advection as the mass transport mechanism, into the characteristic pure extension fractures of this vein group (Figs 6d, 7d).

The evolution of the younger fluid flow system could be positively compared with the general deformation histories of orogens which are often related to a late extensional phase and characterized by an opening of fluid pathways (Conti *et al.* 2001; Gray, Anastasio & Holl, 2001). Fluid migration along faults and open fractures from deeper seated sediments containing radiogenic Sr is proposed to explain higher $^{87}Sr/^{86}Sr$ ratios in hydrothermal calcite veins in an accretionary wedge (Sample & Reid, 1998).

Microthermometric data of fluid inclusions may indicate the lateral and upward migration of hot fluids and precipitation of calcites at more elevated temperatures than the surrounding host-rock. However, due the uncertainties in the pressure correction of the homogenization temperature and the large overlap in the temperature range derived from the conodont alteration index, the vitrinite reflectance, the illite crystallinity and the microthermometry, no evidence for such elevated fluid temperatures in the Moravian Karst area can be deduced from the microthermometric study. The large overlap of the temperatures obtained both from the veins (T_t) and from the host rocks by other methods (CAI, illite crystallinity, R_r) indicates that the studied Variscan veins formed close to maximum temperature and possibly burial conditions. An exception could be veins of group C. They precipitated together with A and B veins in a relatively narrow range of temperatures. While A and B display ductile and brittle–ductile behaviour, the C veins filled only simple fractures formed during brittle fracturing in a pure extension regime. Moreover, the C veins still display nearly the same temperature conditions that influenced host rocks as well. No decreasing trend in temperature can be deduced from the data as the hydrothermal system evolved towards the more open one when fluids migrated through open fractures and structural discontinuities. Considering this, we can speculate that this stage of veining occurred during extension of the crust (Dallmeyer, Franke & Weber, 1995; Zulauf *et al.* 1997). An expanded space for fluid migration must affect a pressure regime. When fracture space is interconnected, the pressure of fluid could fluctuate close to the hydrostatic pressure (e.g. Sibson, 2000). Assuming *P–T* conditions close to hydrostatic (Fig. 9) and the lower pressure derived from this, the C veins could have precipitated at the same depth as the older veins or a little higher in the crust.

Whether the depth of vein (A–B–C) precipitation corresponds to the maximum burial is an open question. However, the presented depths are reasonable when compared with the uplift and denudation for this region reported by Franců *et al.* (2002).

The formation of the calcite veins at relatively low temperatures mainly between 120 and 170 °C and at a maximum depth of 3.2 km corresponds well with the published data on the geotectonic position of the area investigated. The Moravian Karst area was situated far from the Variscan collision zone, with its centre in the northern areas of the Moravo-Silesian Palaeozoic, where even magmatic events were recorded (Dvořák & Přichystal, 1982; Nöth, Karg & Littke, 2001). Maximum vitrinite reflectance data from reworked Palaeozoic sediments in the latter region are up to 9 %, reflecting the intense Variscan tectonism (Kumpera & Martinec, 1995). The Moravo-Silesian Palaeozoic represents the central part of the complex oblique collision of the Variscan accretion wedge with the East Silesian microcontinent in the northeast. This collision took place late in the Variscan tectogenesis (Grygar & Vavro, 1994; Grygar *et al.* 2002).

10. Conclusions

The Variscan fluid system in the Moravian Karst occurred close to maximum burial conditions, and syntectonic calcite veins precipitated during Variscan deformation. The oldest type of vein cement investigated is white calcites that often precipitated in tension gashes during folding and shearing. They crystallized in a geochemically closed system (rock-buffered fluid system) from a relatively low-salinity H_2O–NaCl fluid derived from surrounding host-rocks and with diffusion as a principal mechanism of mass transport. Precipitation most likely took place between 120 and 170 °C, at a lithostatic pressure between 580 and 880 bar (2.1–3.2 km). A younger generation of rose calcite veins precipitated in an open fluid system. The ambient fluid was similar to that from which the white calcites formed. The fluids are likely formation waters present in the sedimentary basin and possibly in the underlying basement. Rose calcites crystallized in the same temperature interval as the white calcites, although possibly at the pure extensional regime, and hence we can speculate that this took place at a lower pressure (300–500 bar) at a depth of 2.1–3.5 km.

The syntectonic fluid system gradually developed from closed rock-buffered to a more open fluid-buffered system. Fluid flow was confined firstly to bed-scale migration, and later the system was active at the scale of the Palaeozoic sedimentary sequence.

The rather low *P–T* conditions during calcite formation are in agreement with the distal position of the Moravian Karst, far from regions of intense Variscan deformation at the north of the Moravo-Silesian Palaeozoic.

Acknowledgements. Financial support for this research was provided in part by the grant GAČR 205/00/0356 and MSM0021622412. We would like to thank V. Hurai for stimulating discussions and G. R. J. Browning for a critical reading and improving English. H. Nijs kindly prepared the doubly polished wafers. The comments of R. Shail and an anonymous referee provided helpful critical reviews.

References

ABART, R. & RAMSEYER, K. 2002. Deformation induced quartz-fluid oxygen isotope exchange during low-grade metamorphism: an example from the Glarus thrust, E Switzerland. *Schweizerische Mineralogische und Petrographische Mitteilungen* **82**, 291–302.

BADERTSCHER, N. P., ABART, R., BURKHARD, M. & MCCAIG, A. 2002. Fluid flow pathways along the Glarus overthrust derived from stable and Sr-isotope patterns. *American Journal of Science* **302**, 517–47.

BARKER, CH. & GOLDSTEIN, R. H. 1990. Fluid-inclusions technique for determining maximum temperature in calcite and its comparison to the vitrinite reflectance geothermometer. *Geology* **18**, 1003–6.

BARNABY, R. J. & RIMSTIDT, J. D. 1989. Redox conditions of calcite cementation interpreted from Mn and Fe contents of authigenic calcites. *Geological Society of America Bulletin* **101**, 795–804.

BODNAR, R. J. 1993. Revised equation and table for determining the freezing point depression of H_2O–NaCl solutions. *Geochimica et Cosmochimica Acta* **57**, 683–4.

BONI, M., PARENTE, G., BECHSTADT, T., DE VIVO, B. & IANNACE, A. 2000. Hydrothermal dolomites in SW Sardinia (Italy): evidence for a widespread late-Variscan fluid flow event. *Sedimentary Geology* **131**, 181–200.

BONS, P. D. 2001. The formation of large quartz veins by rapid ascent of fluids in mobile hydrofractures. *Tectonophysics* **336**, 1–17.

BORISENKO, A. S. 1977. Izucenie solevovo sostava rastvorov gazovo-zidkih vklucenij v mineralah metodom kriometrii. *Geologija i Geofizika* **8**, 16–27. Novosibirsk: Akademija Nauk SSSR, Sibirskoe otdelenije (in Russian).

BROCHWICZ-LEWINSKI, W., VIDAL, G., POZARYSKI, W., TOMCZYK, H. & ZAJAC, R. 1986. Pre-Permian tectonic position of the Upper Silesian Massif (S Poland) in the light of studies on the Cambrian. *Comptes Rendus de l'Académie des Sciences, Série 11* **303**, 1493–6.

BUDD, D. A., HAMMES, U. & WARD, W. B. 2000. Cathodoluminescence in calcite cements: New insights on Pb and Zn sensitizing, Mn activation, and Fe quenching at low trace-element concentrations. *Journal of Sedimentary Research* **70**, 217–26.

BURKHARD, M. & KERRICH, R. 1988. Fluid regimes in the deformation of the Helvetic nappes, Switzerland, as inferred from stable isotope data. *Contributions to Mineralogy and Petrology* **99**, 416–29.

CANOLE, P., ODONNE, F. & POLVE, M. 1997. Heterogeneous strain associated with normal faulting: evidence of mass transfer by pressure solution associated with fault displacement. *Tectonophysics* **283**, 129–43.

CARTWRIGHT, I. & BUICK, I. S. 2000. Fluid generation, vein formation and the degree of fluid-rock interaction during decompression of high-pressure terranes: the Schistes Lustres, Alpine Corsica, France. *Journal of Metamorphic Geology* **18**, 607–24.

CONTI, A., TURPIN, L., POLINO, R., MATTEI, M. & ZUPPI, G. M. 2001. The relationship between evolution of fluid chemistry and the style of brittle deformation: examples from the Northern Apennines (Italy). *Tectonophysics* **330**, 103–17.

COSTAGLIOLA, P., BENVENUTI, M., MAINERI, C., LATTANZI, P. & RUGGIERI, G. 1999. Fluid circulation in the Apuane Alps core complex: evidence from extension veins in the Carrara marble. *Mineralogical Magazine* **63**, 111–22.

CRAIG, H. 1957. Isotopic standards for carbon and oxygen correction factors for mass spectrometric analysis for carbon dioxide. *Geochimica et Cosmochimica Acta* **12**, 133–49.

DALLMEYER, R. D., FRANKE, W. & WEBER, K. (eds) 1995. *Pre-Permian Geology of Central and Eastern Europe*. Berlin: Springer Verlag, 604 pp.

DUDEK, A. 1980. The crystalline basement block of the Outer Carpathians in Moravia – Brunovistulicum. *Rozpravy Československé Akademie věd, řada matematických a přírodních věd* **90**, 8, 1–85. Prague.

DUNNE, W. M. 1986. Mesostructural development in detached folds: an example from West Virginia. *Journal of Geology* **94**, 473–88.

DVOŘÁK, J. 1990. Paleofacial and paleoclimatic aspects of the Devonian and Carboniferous sedimentation in the Rhenohercynicum and Moravia. *Věstník Ústředního Ústavu geologického* **65**, 65–74. Prague.

DVOŘÁK, J. & PŘICHYSTAL, A. 1982. Lamprofyry stefanského stáří Janovsko-Artmanovského antiklinoria ve Slezsku. *Sborník geologických Věd, Geologie* **36**, 93–113. Prague (in Czech).

DVOŘÁK, J., HONĚK, J., PEŠEK, J. & VALTEROVÁ, P. 1997. Deep borehole evidence for a southward extension of the Early Namurian deposits near Němčičky, S. Moravia, Czech Republic: implication for rapid coalification. In *European Coal Geology and Technology* (eds R. Gayer and J. Pešek), pp. 179–93. Geological Society of London, Special Publication no. 125.

DVOŘÁK, J. & PTÁK, J. 1963. Geologický vývoj a tektonika devonu a spodního karbonu Moravského krasu. *Sborník geologických Věd, Geologie* **3**, 49–77. Prague (in Czech).

DVOŘÁK, J. & SKOČEK, V. 1975. Reconstruction of the paleoheat flow regime in two areas of the Variscan orogene. *Neues Jahrbuch fur Geologie und Palaontologie, Monatshefte* **H. 9**, 517–27.

EPPEL, H. & ABART, R. 1997. Grain-scale stable isotope disequilibrium during fluid-rock interaction; 2, An example from the Penninic–Austroalpine tectonic contact in eastern Switzerland. *American Journal of Science* **297**, 707–28.

EVANS, M. A. & BATTLES, D. A. 1999. Fluid inclusion and stable isotope analyses of veins from the central Appalachian Valley and Ridge province: implications for regional synorogenic hydrologic structure and fluid migration. *Geological Society of America Bulletin* **111**, 1841–60.

FERKET, H., SWENNEN, R., ORTUNO, S. & ROURE, F. 2003. Reconstruction of the fluid flow history during Laramide foreland fold and thrust belt development in eastern Mexico: cathodoluminescence and δ^{18}O– δ^{13}C isotope trends of calcite-cemented fractures. *Journal of Geochemical Exploration* **78–79**, 163–7.

FINGER, F., HANŽL, P., PIN, C., QUADT, A. & STEYRER, H. P. 2000. The Brunovistulicum: Avalonian Precambrian at the eastern end of the Variscides. In *Orogenic Processes: Quantification and Modelling in the Variscan Belt of Central Europe* (eds W. Franke, R. Altherr, W. Haak, O. Oncken and D. Tanner), pp. 103–13. Geological Society of London, Special Publication no. 179.

FITZGERALD, E., FEELY, M., JOHNSTONE, J. D., CLAYTON, G., FITZGERALD, L. J. & SEVASTOPULO, G. D. 1994. The Variscan thermal history of West Clare, Ireland. *Geological Magazine* **131**, 545–58.

FRANCŮ, E., FRANCŮ, J. & KALVODA, J. 1999. Illite crystalinity and vitrinite reflectance in Paleozoic siliciclastics in the SE Bohemian Massif as evidence of thermal history. *Geologica Carpathica* **50**, 365–72.

FRANCŮ, E., FRANCŮ, J., KALVODA, J., POELCHAU, H. S. & OTAVA, J. 2002. Burial and uplift history of the Palaeozoic flysch in the Variscan foreland basin (SE Bohemian Massif, Czech Republic. In *Continental collision and the tectonosedimentary evolution of forelands* (eds G. Bertotti, K. Schulmann, and S. Cloetingh), pp. 259–78. European Geophysical Society, Stephan Mueller Special Publication Series, Vol. 1.

FRANCŮ, E., KALVODA, J., FRANCŮ, J., POELCHAU, H. S. & OTAVA, J. 1998. Thermal history of the Paleozoic in the SE Bohemian Massif in respect to Variscan orogeny. *Acta Universitatis Carolinae, Geologica* **42**, 247–8.

FRANKE, W., DALLMEYER, R. D. & WEBER, K. 1995. XI Geodynamic evolution. In *Pre-Permian Geology of Central and Eastern Europe* (eds R. D. Dallmeyer, W. Franke and K. Weber), pp. 579–94. Berlin: Springer Verlag.

FRITZ, H. & NEUBAUER, F. 1993. Kinematics of crustal stacking and dispersion in the south-eastern Bohemian Massif. *Geologische Rundschau* **82**, 556–65.

GOLDSTEIN, R. H. 1986. Reequilibration of fluid inclusions in low-temperature calcium-carbonate cement. *Geology* **14**, 792–5.

GRAY, D. R., GREGORY, R. T. & DURNEY, D. W. 1991. Rock-buffered fluid-rock interaction in deformed quartz-rich turbidite sequences, Eastern Australia. *Journal of Geophysical Research* **96**, 19681–704.

GRAY, E. B., ANASTASIO, D. J. & HOLL, J. E. 2001. Synorogenic crustal fluid infiltration in the Idaho–Montana thrust belt. *Geophysical Research Letters* **28**, 4295–8.

GREGORY, R. T. & CRISS, R. E. 1986. Isotopic exchange in open and closed systems. In *Stable isotopes in higher temperature geologic processes* (eds J. W. Walley, H. P. Taylor and J. R. O'Neil), pp. 91–127. Reviews in Mineralogy, vol. 16. Mineralogical Society of America.

GRYGAR, R., GNOJEK, I., HUBATKA, F. & JELÍNEK, J. 2002. Brunovistulian terrane – synthesis of morphostructural analysis and geophysical data (Moravo-Silesian area, Czech republic). *Geolines* **14**, 26–7. Prague.

GRYGAR, R. & VAVRO, M. 1994. Geodynamic model of evolution of Lugosilesian orocline of European Variscan orogeny belt. *Journal of Czech Geological Society* **39**, 40–1.

HANŽL, P., KREJČÍ, Z., VÍT, J., OTAVA, J., NOVÁK, Z. & STRÁNÍK, Z. 1999. *Geological map of Brno City and its surroudings, 1:50 000*. Czech Geological Survey, Prague.

HILGERS, CH. & URAI, J. L. 2002. Microstructural observations on natural syntectonic fibrous veins: implications for the growth process. *Tectonophysics* **352**, 257–74.

HLADIL, J. 1991. Násuny v jižním uzávěru Moravského krasu (mapový list 24-413 Mokrá-Horákov). *Zprávy o geologických výzkumech v r. 1989*, 80–1. Czech Geological Survey, Prague (in Czech).

HLADIL, J., KREJČÍ, Z., KALVODA, J., GINTER, M., GALLE, A. & BEROUŠEK, P. 1991. Carbonate ramp environment of Kellwasser Time-Interval (Lesní lom, Moravia, Czechoslovakia). *Bulletin de la Société belge de Géologie* **100**, 57–119.

HLADIL, J., MELICHAR, R., OTAVA, J., GALLE, A., KRS, M., MAN, O., PRUNER, P., CEJCHAN, P. & OREL, P. 1999. The Devonian in the easternmost Variscides, Moravia: a holistic analysis directed towards comprehension of the original context. *Abhandlungen der Geologischen Bundesanstalt* **54**, 27–47.

HROUDA, F. 1981. On the superposition of the regional slaty cleavage on folded strata and its reflection in magnetic anisotropy. *Časopis pro mineralogii a geologii* **26**, 341–8. Prague.

JAMTVEIT, B. & YARDLEY, B. W. D. 1997. Fluid flow and transport in rocks: an overwiev. In *Fluid flow and transport in rocks* (eds B. Jamtveit and B. W. D. Yardley), pp. 1–14. London: Chapman and Hall.

JANSSEN, C., LAUBE, N., BAU, M. & GRAY, D. R. 1998. Fluid regime in faulting deformation of the Waratah Fault Zone, Australia, as inferred from major and minor element analyses and stable isotopic signatures. *Tectonophysics* **294**, 109–30.

KALVODA, J., MELICHAR, R., BÁBEK, O. & LEICHMANN, J. 2002. Late Proterozoic–Palaeozoic tectonostratigraphic development and palaeogeography of Brunovistulian terrane and comparison with other terranes at the SE margin of Baltica–Laurussia. *Journal of Czech Geological Society* **47**, 81–102.

KAPPLER, P. & ZEEH, S. 2000. Relationship between fluid flow and faulting in the Alpine realm (Austria, Germany, Italy). *Sedimentary Geology* **131**, 147–62.

KENIS, I., MUCHEZ, PH., SINTUBIN, M., MANSY, J. L. & LACQUEMENT, F. 2000. The use of a combined structural, stable isotope and fluid inclusion study to constrain the kinematic history at the northern Variscan front zone (Bettrechies, northern France). *Journal of Structural Geology* **22**, 589–602.

KETTNER, R. 1942. Nové pojetí tektonické stavby Moravského krasu. *Věda přírodní* **21**(2), 33–40. Prague (in Czech).

KIRSCHNER, D. L. & KENNEDY, L. A. 2001. Limited syntectonic fluid flow in carbonate-hosted thrust faults of the Front Ranges, Canadian Rockies, inferred from stable isotope data and structures. *Journal of Geophysical Research – Solid Earth* **106**, 8827–40.

KNOOP, S. R., KENNEDY, L. A. & DIPPLE, G. M. 2002. New evidence for syntectonic fluid migration across the hinterland–foreland transition of the Canadian Cordillera. *Journal of Geophysical Research – Solid Earth* **107 (B4)**, art. no. 2071. DOI 10.1029/2001JB000217.

KRS, M., HLADIL, J., KRSOVÁ, M. & PRUNER, P. 1995. Paleomagnetický doklad pro variskou paleotektonickou rotaci moravských devonských hornin. *Geologické výzkumy na Moravě a ve Slezsku v r. 1994* **2**, 53–7. Brno (in Czech).

KUMPERA, O. & MARTINEC, P. 1995. The development of the Carboniferous accretionary wedge in the Moravian–Silesian Paleozoic basin. *Journal of Czech Geological Society* **40**, 47–64. Prague.

LEISCHNER, K., WELTE, D. H. & LITTKE, R. 1993. Fluid inclusions and organic maturity parameters as calibration tools in basin modelling. In *Basin modelling: advances and applications* (eds A. G. Doré, J. H. Augustson, C. Hermanrud, D. J. Stewart and Ø. Sylta), pp. 161–72. Amsterdam: Norwegian Petroleum Society.

LOSH, S. 1997. Stable isotope and modeling studies of fluid-rock interaction associated with the Snake Range and Mormon Peak detachment faults, Nevada. *Geological Society of America Bulletin* **109**, 300–23.

LÜNENSCHLOSS, B. 1998. *Modellierung der Temperature- und Fluidgeschichte an der variszischen Front (Verviers-Synklinorium und Nordeifel)*. Scientific Technical Report GeoForschungsZentrum Potsdam STR 98/07.

MALKOVSKÝ, M. 1978. Neoidic mineralization in the Bohemian Massif associated with the Saxon tectogenesis. *Věstník Ústředního Ústavu geologického* **53**(3), 129–44. Prague.

MARQUER, D. & BURKHARD, M. 1992. Fluid circulation, progressive deformation and mass-transfer processes in the upper crust: the example of basement-cover relationships in the External Crystalline Massifs, Switzerland. *Journal of Structural Geology* **14**, 1047–57.

MATHIEU, R., PAGEL, M., CLAUER, N., DE WINDT, L., CABRERA, J. & BOISSON, J. Y. 2000. Paleocirculations in shales: a mineralogical and geochemical study of calcite veins from the Tournemire tunnel site (Aveyron, France). *European Journal of Mineralogy* **12**, 377–90.

MEERE, P. A. & BANKS, D. A. 1997. Upper crustal fluid migration: an example from the Variscides of SW Ireland. *Journal of Geological Society, London* **154**, 975–85.

MELICHAR, R. & KALVODA, J. 1997. Stavba a geologická charakteristika Němčicko-Vratíkovského pruhu. *Proceedings of Second Workshop of the Czech Group for Tectonic Studies* **2**, 51–2. Ostrava (in Czech).

MICARELLI, L., BENEDICTO, A., INVERNIZZI, C., SAINT-BEZAR, B., MICHELOT, J. L. & VERGELY, P. 2005. Influence of P/T conditions on the style of normal fault initiation and growth in limestones from the SE-Basin, France. *Journal of Structural Geology* **27**(9), 1577–98.

MUCHEZ, PH. & SINTUBIN, M. 1998. Contrasting origin of palaeofluids in a strike-slip fault system. *Chemical Geology* **145**, 105–14.

MUCHEZ, PH., SLOBODNÍK, M., VIAENE, W. A. & KEPPENS, E. 1995. Geochemical constraints on the origin and migration of palaeofluids at the northern margin of the Variscan foreland, southern Belgium. *Sedimentary Geology* **96**, 191–200.

MUSIL, R. 1993. *Moravský kras – labyrinty poznání. Adamov*. J. Bližňák, 336 pp. (in Czech).

NEMČOK, M., HENK, A., GAYER, R. A., VANDYKE, S. & HATHAWAY, M. 2002. Strike-slip fault bridge fluid pumping mechanism: insights from field-based palaeostress analysis and numerical modeling. *Journal of Structural Geology* **24**, 1885–1901.

NESBITT, B. E. & MUEHLENBACHS, K. 1989. Origins and movement of fluids during deformation and metamorphism in the Canadian Cordillera. *Science* **245**, 733–6.

NESBITT, B. E. & MUEHLENBACHS, K. 1997. Paleohydrogeology of Late Proterozoic units of southeastern Canadian Cordillera. *American Journal of Science* **297**, 359–92.

NÖTH, S., KARG, H. & LITTKE, R. 2001. Reconstruction of Late Paleozoic heat flows and burial histories at the Rhenohercynian–Subvariscan boundary, Germany. *International Journal of Earth Sciences (Geologische Rundschau)* **90**, 234–56.

O'HARA, K. D., YANG, X. Y., GUOYUAN, X. & LI, Z. 1997. Regional $\delta^{18}O$ gradients and fluid-rock interaction in the Altay accretionary complex, northwestern China. *Geology* **25**, 443–6.

OLIVER, N. H. S. & BONS, P. D. 2001. Mechanisms of fluid flow and fluid–rock interaction in fossil metamorphic hydrothermal systems inferred from vein-wallrock patterns, geometry and microstructure. *Geofluids* **1**, 137–62.

O'REILLY, C. & PARNELL, J. 1999. Fluid flow and thermal histories for Cambrian–Ordovician platform deposits, New York: evidence from fluid inclusion studies. *Geological Society of America Bulletin* **111**, 1884–96.

OREL, P. 1996. Stavba evropských variscid ve vztahu k problematice rozpadu řídících litosférických desek a paleotektonickým rotacím s ohledem na východní okraj Českého masivu. *Geologické výzkumy na Moravě a ve Slezsku v r. 1995* **3**, 109–11. Brno (in Czech).

PAGEL, M., BARBIN, V., BLANC, P. & OHNENSTETTER, D. 2000. *Cathodoluminescence in Geosciences*. Berlin: Springer Verlag.

PREZBINDOWSKI, D. R. & LARESE, R. E. 1987. Experimental stretching of fluid inclusions in calcite – Implications for diagenetic studies. *Geology* **15**, 333–6.

RAJLICH, P. 1987. *Tektonika duktilních domén Českého masivu*. Prague: Czech Geological Survey, 82 pp. (in Czech).

RAJLICH, P. 1990. Strain and tectonic styles related to Variscan transpression and transtension in the Moravo-Silesian Culmian basin, Bohemian Massif, Czechoslovakia. *Tectonophysics* **174**, 351–7.

RAJLICH, P., SLOBODNÍK, M. & NOVOTNÝ, A. 1989. Variscan crustal boudinage in the Bohemian Massif: gravimetry, magnetometry and structural data from the Desná dome. *Jahrbuch der Geologischen Bundesanstalt* **132**(1), 241–6. Wien.

RAMSAY, J. G. 1980. The crack-seal mechanism of rock deformation. *Nature* **284**, 135–9.

RAMSAY, J. G. & HUBER, M. I. 1987. *The Techniques of Modern Structural Geology. Volume 2: Folds and Fractures*. New York: Academic Press.

RENARD, F., GRATIER, J. P. & JAMTVEIT, B. 2000. Kinetics of crack-sealing, intergranular pressure solution, and compaction around active faults. *Journal of Structural Geology* **22**, 1395–1407.

RICHARDS, I. J., CONNELLY, J. B., GREGORY, R. T. & GRAY, D. R. 2002. The importance of diffusion, advection, and host-rock lithology on vein formation: A stable isotope study from the Paleozoic Ouachita orogenic belt, Arkansas and Oklahoma. *Geological Society of America Bulletin* **114**, 1343–55.

SAMPLE, J. C. & REID, M. R. 1998. Contrasting hydrogeologic regimes along strike-slip and thrust faults in the Oregon convergent margin: Evidence from the chemistry of syntectonic carbonate cements and veins. *Geological Society of America Bulletin* **110**, 48–59.

SCHULMANN, K., LEDRU, P., AUTRAU, A., MELKA, R., LARDEAUX, J. M., URBAN, M. & LOBKOWICZ, M. 1991. Evolution of nappes in the eastern margin of the Bohemian Massif: a kinematic interpretation. *Geologische Rundschau* **80**, 73–92.

SCHULZ, B., AUDREN, C. & TRIBOULET, C. 2002. Oxygen isotope record of fluid-rock-SiO_2 interaction during Variscan progressive deformation and quartz veining in the meta-volcanosediments of Belle-Ile (Southern Brittany). *Journal of Structural Geology* **24**, 1281–97.

SIBSON, R. H. 2000. Fluid involvement in normal faulting. *Journal of Geodynamics* **29**, 469–99.

SLOBODNÍK, M., MUCHEZ, PH. & VIAENE, W. 1997. Hydrothermal fluid flow in the Devonian and Carboniferous of the Rhenohercynicum of the Bohemian Massif. In *Mineral Deposits: Research and Exploration – Where do They Meet?* (ed. H. Papunen), pp. 583–6. Rotterdam: A. A. Balkema.

SPENCER, T. K., MØLLER, N. & WEARE, J. H. 1990. The prediction of mineral solubilities in natural waters: A chemical equilibrium model at temperatures below 25°C. *Geochimica et Cosmochimica Acta* **54**, 575–90.

SRIVASTAVA, D. C. & ENGELDER, T. 1990. Crack-propagation sequence and pore-fluid conditions during fault-bend folding in the Appalachian Valley and Ridge, central Pennsylvania. *Geological Society of America Bulletin* **102**, 116–28.

SRIVASTAVA, D. C. & SAHAY, A. 2003. Brittle tectonics and pore-fluid conditions in the evolution of the Great Boundary Fault around Chittaurgarh, Northwestern India. *Journal of Structural Geology* **25**, 1713–33.

STŘELCOVÁ, E., FRANCŮ, J. & POELCHAU, H. S. 1997. Model tepelné historie paleozoika Konicka na základě odraznosti vitrinitu. *Geologické výzkumy na Moravě a ve Slezsku v r. 1996* **4**, 83–5. Brno (in Czech).

TAIT, J. A., BACHTADSE, V. & SOFFEL, H. 1996. Eastern Variscan fold belt: Palaeomagnetic evidence for oroclinal bending. *Geology* **24**, 871–4.

VAN BREEMEN, O., AFTALION, M., BOWES, D. R., DUDEK, A., MÍSAŘ, Z., POVONDRA, P. & VRÁNA, S. 1982. Geochronological studies of the Bohemian Massif, Czechoslovakia, and their significance in the evolution of Central Europe. *Transactions of the Royal Society of Edinburgh, Earth Sciences* **75**, 89–108.

VAN GEET, M., SWENNEN, R., DURMISHI, C., ROURE, F. & MUCHEZ, PH. 2002. Paragenesis of Cretaceous to Eocene carbonate reservoirs in the Ionian fold and thrust belt (Albania): relation between tectonism and fluid flow. *Sedimentology* **49**, 697–718.

WAGNER, T. & COOK, N. J. 2000. Late-Variscan antimony mineralisation in the Rheinisches Schiefergebirge, NW Germany: evidence for stibnite precipitation by drastic cooling of high-temperature fluid systems. *Mineralium Deposita* **35**, 2–3, 206–22.

XU, G. 1997. Fluid inclusions in crack-seal veins at Dugald River, Mount Isa Inlier: implications for palaeostress states and deformation conditions during orogenesis. *Journal of Structural Geology* **19**, 1359–68.

YARDLEY, B. W. D. & LLOYD, G. E. 1989. An application of cathodoluminescence microscopy to the study of textures and reactions in high-grade marbles from Connemara, Ireland. *Geological Magazine* **126**, 333–7.

ZHANG, Y. G. & FRANTZ, J. D. 1987. Determination of the homogenization temperatures and densities of supercritical fluids in the system NaCl–KCl–$CaCl_2$–H_2O using synthetic fluid inclusions. *Chemical Geology* **64**, 335–50.

ZULAUF, G., DORR, W., FIALA, J. & VEJNAR, Z. 1997. Lower Carboniferous lift tectonics in the Bohemian Massif: a special kind of gravitational collapse in thickened orogenic crust. SPP Kolloquium Orogene Prozesse, Bayreuth (March 13–14 1997). *Terra Nostra* **5**, 216–18. Bayreuth.